International Journal of communication and computer Technologies, ISSN: 2278-9723

Available at http://www.ijccts.org

IMPROVING THE GRID PERFORMANCE IN HYBRID RENEWABLE ENERGY SYSTEM

J.Muthupraveen1 and G.Ramakrishnaprabu2 ,

1,2. P.G student, Department of Electrical and Electronics Engineering,

Assistant Professor, Department of Electrical and Electronics Engineering,

VMKV Engineering College, Salem

Received: 16-01-2015, **Revised:** 19-03-2015, **Accepted:** 22-04-2015, **Published online:** 02-06-2016

ABSTRACT

This paper proposes the performance analysis and regulation of hybrid standalone energy system. In this hybrid system consist of wind turbine, fuel cell, electrolyzer, battery and a set of loads. The system having two level structures. Here the top level is Energy management and power regulation system (EMPRS), and the low level is individual subsystem. The dynamic operating point is set by wind and load condition. By using this reference point the individual subsystem operates and the local controllers control the fuel cell, wind turbine, electrolyzer, and battery storage. This control structure is implemented in MATLAB Simpower software.

Key word- Battery storage, electrolyzer, energy management and power regulation system, fuel cell, load management, stand-alone hybrid energy system, wind energy conversion system.

I. INTRODUCTION:

In the remote area, diesel generator is commonly used for power generation because grid connections are not often available and its installation cost is low and more reliability [1], [2]. The diesel generator causes more pollution to environment.

The hybrid power generation combines with a different renewable energy sources and it is

environment friendly. Renewable energy system has appropriate control and coordination strategies among various elements. It is reliable and cost effective [3].

There are different types of renewable energy sources such as solar, wind, biomass, geothermal, tidal, and fuel cell, e.t.c. In this hybrid stand-alone energy system consists of wind, fuel cell, electrolyzer, battery storage.

The system that consisting of solar and wind are not more efficient. Due to solar (PV) pannel and it will be giving less efficiency. Here they have used three power management strategies but it is not more efficient [4]. For controlling the heavy wind condition and its reducing fluctuation of wind is seen [5].

In the grid connected wind generator, the control strategy used is pi controller they build up to provide some ancillary service to grid. Here the source following is more efficient than the grid following [6]. The ultra capacitor are not used due to high cost and also the cost of hydrogen is also too high [7].

The system that consists of converter, inverter unit and for stand-alone application and it has more losses [8]. The case study of the

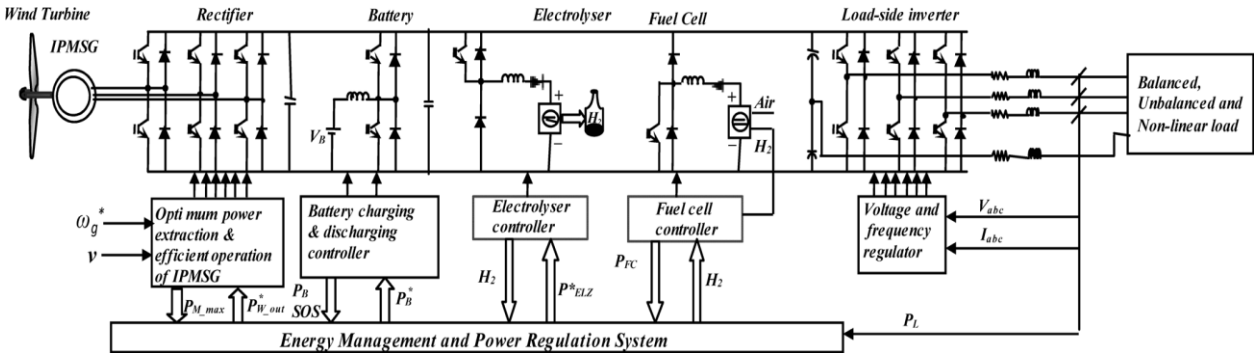

Fig. 1. Structure of the proposed hybrid power generation system.

energy management of fuel cell and battery for hybrid tram way [9]. Recent studies on the hybrid power system focus on various issues such as cost optimization and size [10].

This paper proposes about improve regulation and performance of hybrid stand alone energy system. In this EMPRS is using for control and flexibility for various wind conditions and it prevents the system block out.

Based on the dynamic operating point each subsystem is controlled. The fuel cell is controlled by the hydrogen flow regulator and the boost converter. The electrolyzer is controlled by the buck converter. And the battery is controlled by the Bi directional dc-dc converter.

II SYSTEM COMPONENTS AND CONTROLLER MODELLING:

A) Wind Energy Conversion System (WECS) Modeling:

1) Wind Turbine Model for Optimum Energy Extraction: The aerodynamic rotor power from wind (Pw) can be expressed as [11]

$$Pw=0.5A\rho CP(\lambda, \beta)\, v3;\ v0>v>VI \quad .....(1)$$

Where ρ is the air density, A is the rotor swept area, V is the wind speed, V0 and Vi are the cut-in and cut-off wind speed, respectively, and CP is the power coefficient which is a function of the speed ratio λ and the pitch angle β.

The speed ratio of the wind turbine can be defined as

$$\lambda=\omega rR/V \quad ..... (2)$$

Where ωr is the rotor speed and R is the radius of rotor.

From (1) and (2), for a particular wind speed, the output power is proportional to the rotor speed and can be expressed as

$$PW = K\omega r3 \quad ..... (3)$$

Where $K=0.5A\rho CP(R/\lambda)\,3$

From (3), optimum aerodynamic rotor power from the wind turbine can be extracted by controlling the rotor speed. For (ωr) a particular wind speed, the optimum power is given as [11]

$$PWopt = Kopt\ \omega r3 \quad ..... (4)$$

Where $K=0.5A\rho CPopt(R/\lambda opt)\,3$

Demonstrates the power generated by a turbine as a function of the rotor speed for different wind speeds. The optimum power extraction from the wind refers to extracting the necessary power under varying wind speed conditions. As an example, for a particular wind speed (V6), the optimum power (PWopt) is generated by keeping the rotor speed equal to either ω1 or ω3. However, as ω3 is higher than the base rotor speed ω1, the control system has to choose the rotor speed. If the wind speed drops from V6 to V5, the control system sets the rotor speed to ω2 to extract the required power.

2) IPM Synchronous Generator Model: The voltage equations of the IPM synchronous generator in the -and -axes are expressed as follows [12]:

$$Vd = idRs + Ld\ d/dt\ (id) - \omega Lqiq \quad ..... (5)$$

$$Vq = iqRs + Lq\ d/dt\ (iq) + \omega Ldid + \omega\varphi f \quad .... (6)$$

Improving the Grid Performance in Hybrid Renewable Energy System

Where Vd and Vq are the d- and q-axes components of the stator voltage, respectively; Rs is the stator resistance; id and iq are the d- and q- axes components of the stator current, respectively; ω is the frequency; and φf is the flux linkage.

The torque equation of the IPM synchronous generator can be expressed as follows [12]:

Tg = -3/2 Pn{φfiq+(Ld- Lq) idiq……. (7)

Where Pn is the number of pole pairs, and Tg is the generated torque of the IPM synchronous generator.

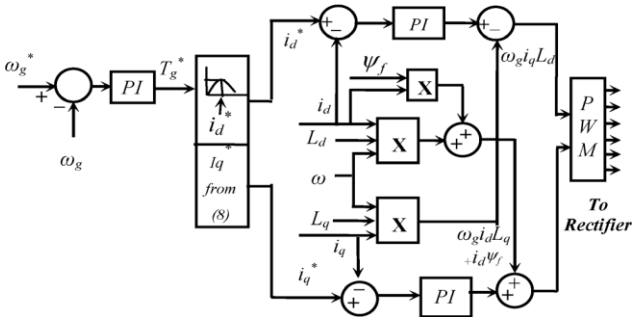

Fig:2 Machine side converter controller

From (7), the q-axis stator current component for constant torque can be expressed as a function of the d-axis stator current component

$$i_q = \frac{-2Tg}{3Pn\{\varphi f + (Ld - Lq) id} \quad \ldots\ldots(8)$$

The maximum efficiency of the IPM synchronous generator can be achieved by minimizing the copper and core losses. From Fig. 3, the copper (Pcu) and the core (Pcore) losses for the IPM synchronous generator can be determined as follows [13]:

$$P_{cu} = Rs(i_d^2 + i_q^2) \quad \ldots\ldots\ldots(9)$$

$$P_{core} = \frac{\square 2\{(Ldid+\varphi f)2+(Lqiq)2}{Rc} \quad \ldots.. (10)$$

Where Rc is the core loss component.

The output power from the generator can be given as

$$P_{out} = P_W - P_{cu} - P_{core}$$

$$= T_g - R_s(i_d^2 + i_q^2) - \frac{\square 2\{(Ldid+\varphi f)2+(Lqiq)2}{Rc} \ldots(11)$$

The optimum value of id can be determined from the output power (Pout) versus the d-axis stator current (id) curve based on (5)–(11), as shown in Fig. 4. From Fig. 4, the optimum value of the d- axis current component is chosen such that the output power of the IPM synchronous generator is maximized. The corresponding value of id can be obtained from (8).

3) Machine Side Converter Controller Design:

The machine side converter shown in Fig. 2 consists of three PI controllers working on the principle based on (5)–(11). In the first stage, PI controller is used to regulate the speed by controlling the torque. In the second stage, two PI controllers are used to regulate the d- and q - axes currents under specific torque or power conditions in order to minimize losses.

B. Fuel Cell Model and Control

The model used in the paper is based on the dynamic proton exchange membrane fuel cell model (PEMFC) discussed in [14] and [15].

This model is based on a relationship between the Nernst voltage and the average magnitude of the fuel cell stack voltage [14].

VFC= N0E-Vloss ……. (12)

Where VFC is the fuel cell voltage, N0 is the number of fuel cells connected in series, E is the Nernst voltage, and Vloss is the irreversible voltage losses.

The Nernst voltage developed in the fuel cell is defined as follows [14]:

$$E = E0 + E^{\frac{RT}{2F}} \ln \frac{PH2P0.5o2}{PH2o} \quad \ldots\ldots\ldots (13)$$

Where E0 is the voltage associated with the reaction free energy, R is the universal gas constant, F is the Faraday's constant, T is the fuel cell absolute temperature, PH2the partial pressure of hydrogen in the anode, PO2 and PH2oare the partial pressure of oxygen and water available in the cathode, respectively.PH2 PO2, and PH2Ocan be expressed using the following differential equations [14]:

$$PH2 = -\frac{1}{TH2}(PH2 + \frac{1}{KH2}(MH2, FC - 2KrIFC))$$

$$PH2O = -\frac{1}{TH2O}(PH2O + \frac{2}{KH2O} KrIFC)$$

PO2= $\frac{1}{TO2}$(PO2+$\frac{1}{KO2}$(MO2,FC-KrIFC)) ……. (14)

Where MH2,FC and MO2,FC are the molar follow of hydrogen and oxygen, respectively; KH2,KH2O, and KO2 are constants; Kr is a constant, which can be defined by the relationship between the rate of reactant hydrogen (qrH2) and IFC is the fuel cell current [14]

qrH2 =2 Kr IFC …… (15)

The output voltage of a fuel cell at normal operating conditions is determined by the irreversible voltage loss (Vloss), which can be classified into three types: the activation voltage

Loss (Vact) , ohmic voltage loss (Vohm) , and concentration voltage loss (Vconc) [12].

The output power of a fuel cell is determined as follows:

PFC=VFCIFC …… (16)

In order to design a control strategy for the fuel cell, the hydrogen flow has to be regulated to achieve the output power based on (12)–(16). Moreover, as the fuel cell voltage varies according to the dynamic operating point, as shown, a controlled boost converter is used to interface the fuel cell with the dc link of the system. The fuel cell controller is shown in Fig. 3.

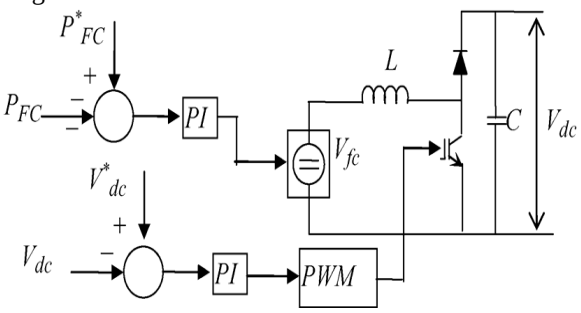

Fig:3 Fuel cell controller

C. Electrolyzer Model and Control

The electrolyzer consumes the electric power to produce hydrogen. The alkaline electrolyzer model is used in the application. The voltage drop across each electrolyzer cell is given by [16], [17]

$u_{cell}=u_0+I_{ELZ}(r_1+r_2T_{ELZ})/A_{ELZ}+u_1\log((t_1+t_2/T_{ELZ}+t_3/T^2_{ELZ})/A_{ELZ}+1)$ …… (17)

Where u_{cell} is the voltage drop across the electrolyzer, u_0 is the thermodynamic cell voltage, T_{ELZ} is the electrolyzer temperature, u_1 and t_{is} are parameters for the electrolyzer over voltage, r_{is} are parameters of ohmic resistance, I_{ELZ} is the electrolyzer current, A_{ELZ} and is the area of electrode.

The total voltage drop (U_{ELZ}) across the electrolyzer is defined as [16]

$U_{ELZ}=N_{ELZ}\, u_{cell}$ ……. (18)

Where N_{ELZ} is the number of cells.

The total power consumption of the electrolyzer is given as

$P_{ELZ}= U_{ELZ}\, I_{ELZ}$ ……. (19)

The electrical characteristics of the electrolyzer depend on the voltage, current, and temperature. The nonlinear relationship of the electrolyzer cell voltage and current at a given temperature is shown.

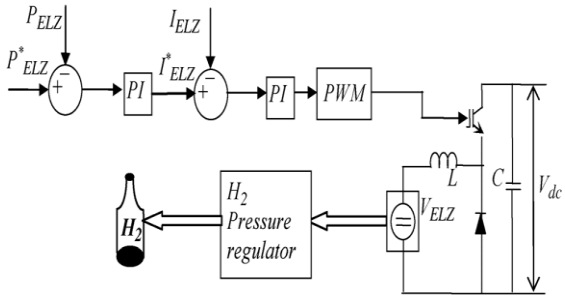

Fig:4 Electrolyzer controller

The hydrogen production rate (MH2,pro) can be expressed as a function of applied current as follows [16], [18]:

MH2,pro=Ƞ(T,J) $\frac{NELZ}{2F}$ IELZ ……(20)

Where F is the Faraday's constant, J is the current density, and Ƞ is a function of the current density and temperature.

In normal operating conditions, the hydrogen outlet rate should be equal to the hydrogen production rate so that the pressure and stored hydrogen quantity in the cathode can be maintained as constant. Based on the ideal gas law, the resultant pressure of hydrogen can be written as [16], [18]

$\frac{\sqcup ELZ}{RTELZ}\frac{d}{dt}p_{H2,ELZ}= M_{H2,pro}-M_{H2,ELZ}$ …..(21)

Where ΘELZ is the cathode volume, pH2,ELZ is the partial pressure of hydrogen in the cathode, MH2,ELZ is the molar hydrogen out flow rate to hydrogen tank, and R is the ideal gas constant.

In order to control the power flow in the electrolyzer, the input current has to be controlled. A buck converter is used to regulate the power flow in the electrolyzer by regulating the electrolyzer current based on (17)–(21) as shown in Fig.4.

D. Compressor and Tank Model

The relationship between the molar flow rate ($M_{H2,ELZ}$) from the electrolyzer and the compressor power (P_{comp}) is given as follows according to the polytrophic model [16], [18]:

$$M_{H2,ELZ}=\frac{\alpha comp}{w} P_{comp}$$

Where

$$w=\frac{kRTELZ}{k-1}[(\frac{ptank}{pELZ})^{\frac{k-1}{k}}-1] \ldots\ldots (22)$$

Where αcomp is the compression efficiency, and w is the polytrophic work, k is the polytrophic coefficient, and ptank is the pressure of storage tank.

Hydrogen storage (MH2,store) is the difference between the hydrogen produced by the electrolyzer(MH2,ELZ) and the hydrogen used by the fuel cell (MH2,FC)as

MH2,store= MH2,ELZ - MH2,FC …….(23)

The pressure of stored hydrogen (pH2) in the hydrogen tank can be derived as

$$\frac{d}{dt}pH2=\frac{RTtank}{\square tank} MH2,store \ldots\ldots..(24)$$

Where Θtank is the hydrogen storage tank volume, R is the ideal gas constant, and Ttank is the temperature of the tank.

E. Battery Storage System Modeling and Control

Among different battery technologies, Li–ion batteries represent a suitable option for fuel-cell-based hybrid energy storage systems due to their high energy density and efficiency, light weight, and good life cycle [19].

The generic Li–ion battery model is used [20]. The battery state of charge (SOC) is an indication of the energy reserve and is expressed as follows [20]:

$$SOC=100(1-\frac{1}{Q}\int ib\, dt)\% \ldots\ldots\ldots(25)$$

Where ib is the battery current, and Q is the battery capacity.

The battery controller is a bidirectional dc–dc converter that stabilizes the dc link voltage during sudden wind and load changes. The controller is shown in Fig.5.

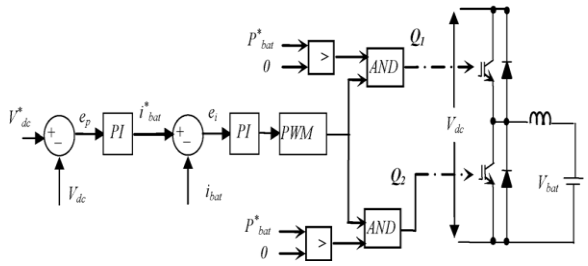

Fig:5 Battery charger/discharger controller

F. Output Voltage and Frequency Controller:

In a standalone power system, various loads (linear, nonlinear, balance, and unbalanced three phase loads) can be connected. As a result, in the proposed system, we use a three phase four wire inverter with split capacitor as shown in Fig.6.

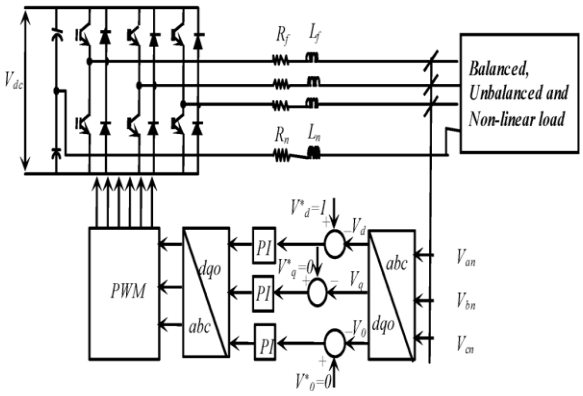

Fig:6 Load side inverter controller

The controller of the inverter compares the d-,q -, and 0-axes components of the output voltage with their reference values (Vd=1,Vq=0,V0=0). Based on the error signal, a set of PI controllers generates appropriate signals to the PWM signal generator.

III SIMULATION RESULTS

The model for the proton exchange membrane (PEM) fuel cell was build in MATLAB/SIMULINK environment.

Experimental setup

The model of 45Vdc, 6kW PEM Fuel Cell Stack connected to a 100Vdc DC/DC converter. The converter is loaded by an RL element of 6kW. The flow rate regulator is bypassed and the rate of fuel is increased to the maximum value of 85 lpm in order to observe the variation in the stack voltage. That will affect the stack efficiency, the fuel consumption and the air consumption.

Fuel cell voltage, current, DC/DC converter voltage and DC/DC converter current signals are available on the Scope2. Fuel flow rate, Hydrogen and oxygen utilization, fuel and air consumption, and efficiency are available on the Scope1.

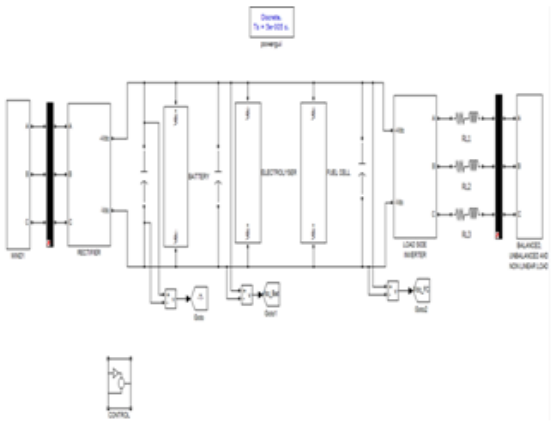

Fig:7 Simulation circuit

The controller of the above simulation circuit is shown below:

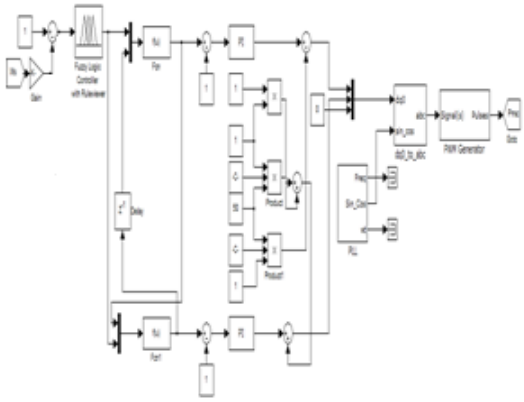

Fig:8 Machine side controller circuit

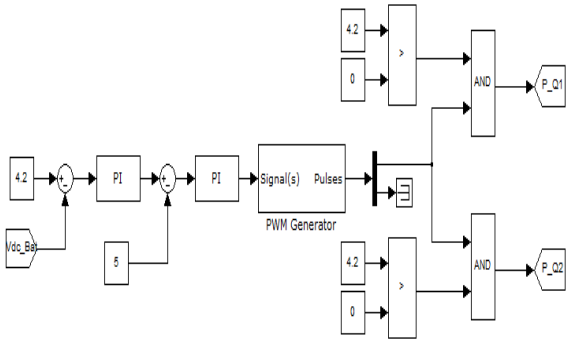

Fig: 9 Battery controller circuit

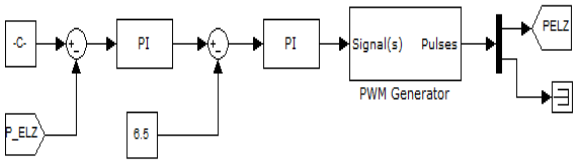

Fig: 10 Electrolyzer controller circuit

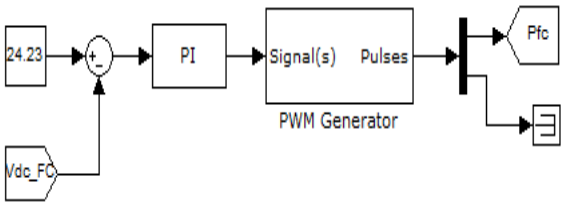

Fig: 11 Electrolyzer controller circuit

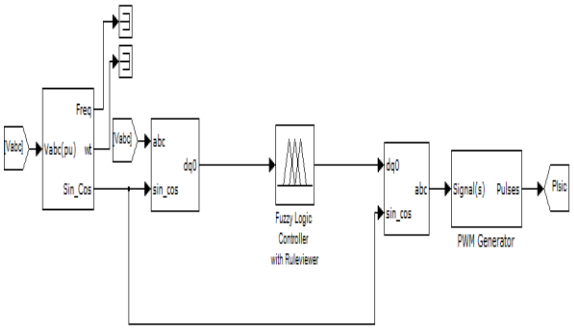

Fig: 12 load side controller circuit

IV SIMULATION RESULT:

The overall output wave form of the above circuit is given below:

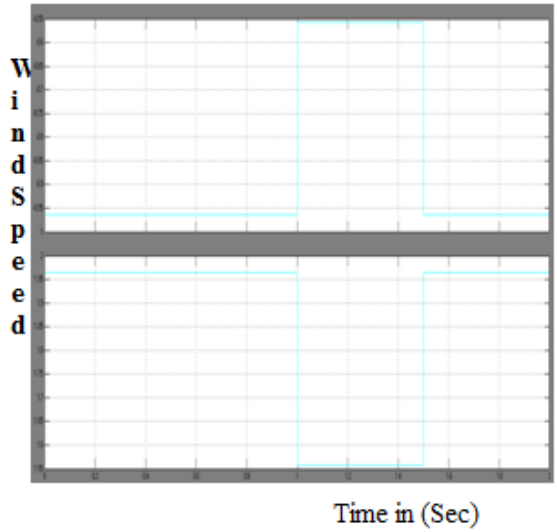

Fig: 13 wind output of first stage

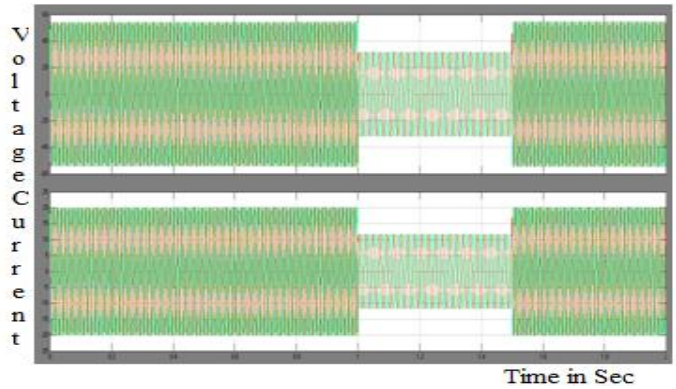

Fig: 14 voltage & current output of wind

From this above figure has the voltage and current. In that, according to the wind speed there will be a change in voltage and current. The current and voltage will be constant from Zero to one (1) second then there will be a fluctuation in the wind so there will be a change in the voltage and current. And there is a small fluctuation in voltage and current for a particular period of time in this for 1.5 second. After that 1.5 second it will go back to its original position and remain constant continuously until there is no fluctuation.

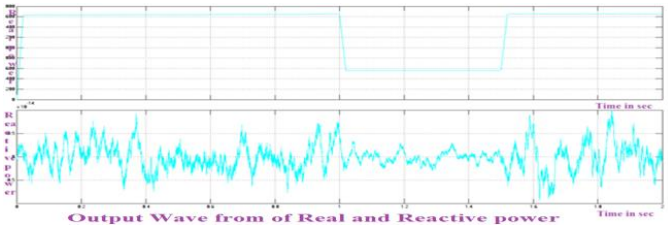

Fig 15 Real and Reactive power output of wind

From this above figure has the real and reactive power. In that, according to the wind speed there will be a change in real and reactive power. The real power will be constant from Zero to one (1) second then there will be a fluctuation in the wind so there will be a change in the real power. And there is a small fluctuation in real power for a particular period of time in this for 1.5 second. After that 1.5 second it will go back to its original position and remain constant continuously until there is no fluctuation. In the reactive power there will be approximately equal to Zero at every time or

some fluctuation up to 0.5 and then it will be come back to zero.

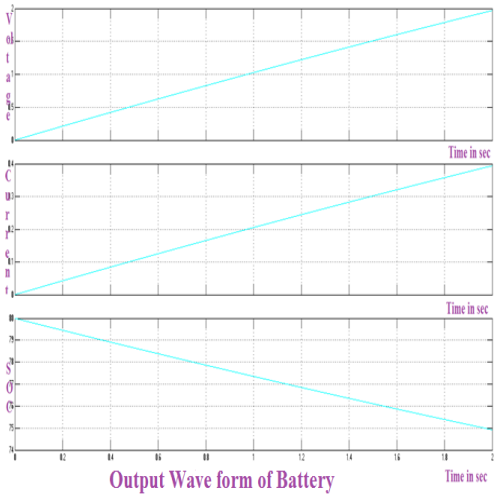

Fig16 output of battery (voltage, current &power)

The above figure consists of voltage, current, state of charge. In this voltage wave form show that the voltage will be constantly increasing from zero up to the maximum range of the circuit. And the current wave form show that the current will be constantly increasing from zero up to the maximum range of the circuit. And the state of charge has the fixed amount of charge and the after a particular period of time it or the graph shows that the wave form will be continuously decreasing then, it shows that the battery discharges until the will be a increased amount of power production in the wind.

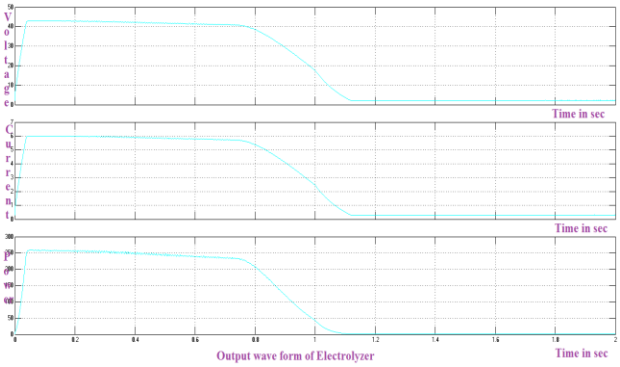

Fig: 17 output of Electrolyzer (voltage, current& power)

The above figure consists of voltage, current, and power. In this voltage wave form show that the voltage will be constant for a particular period of time and then after 1.1 second the voltage will be decreasing and become constant in the circuit. In this Current wave form show that the Current will be constant for a particular period of time and then after 1.1 second the Current will be decreasing and become constant in the circuit. In this power wave form show that the power will be constant for a particular period of time and then after 1.1 second the power will be decreasing and become zero in the circuit.

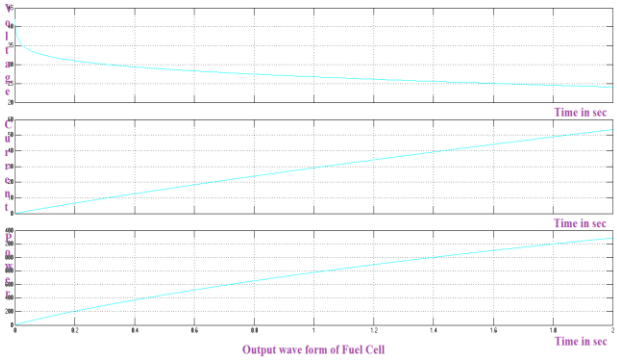

Fig: 18 output of Fuel cell (voltage, current &power)

The above figure consists of voltage, current, and power. In this voltage wave form show that the voltage will be constant for a particular period of time and then after 0.2 second the voltage will be decreasing and become constant voltage in 1.6 second in the circuit and it will be maintained. In this Current wave form show that the Current will be constantly increasing from zero for a particular period of time and then after that period the Current will be maintained constant in the circuit. In this power wave form show that the power will be constantly increasing for a particular period of time and then after that period the power will be maintained constant in that circuit.

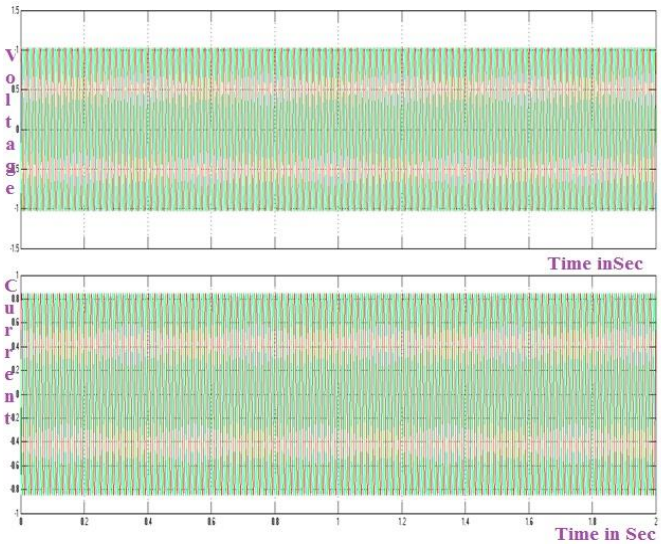

Fig: 19 output of load side inverter (voltage, current)

The above figure consists of voltage, and current. In this voltage wave form show that the voltage will be constant circuit. Because here the fuzzy controller is used to maintain the constant level in the circuit if there is any distortion in the air. In this Current wave form show that the Current will be constant in the circuit. Because here the fuzzy controller is used to maintain the constant level in the circuit if there is any distortion in the air.

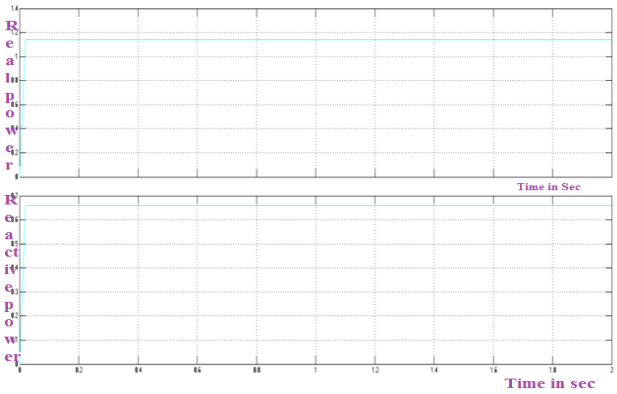

Fig: 20 output of load side inverter (Real and Reactive power)

The above figure consists of Real power and reactive power. In this real power wave form shows that it will be increasing from zero to 0.06 second and maintained constant throughout the circuit, because by using the fuzzy controller in the circuit. In this reactive wave form shows that it will be increasing from zero to 0.06 second and maintained constant throughout the circuit, because by using the fuzzy controller in the circuit.

V CONCLUSION:

The performance analysis and regulation of a hybrid stand alone renewable energy system. From the simulation studies, the fuel cell gives the maximum power during the no/low wind condition. Here the fuel cell used is proton exchange membrane (PEM). The overall coordination is developed by EMPRS. The advantage of EMPRS is to avoid/prevent the system block out at the inadequate energy reserve.

VI REFERENCES:

[1] B. Singh and J. Solanki, "Load compensation for diesel generator- based isolated generation system employing DSTATCOM," *IEEE Trans. Ind. Appl.*, vol. 47, no. 1, pp. 238–244, Jan./Feb. 2011.

[2] R. J. Best, D. J. Morrow, D. J. McGowan, and P. A. Crossley, "Synchronous islanded operation of a diesel generator," *IEEE Trans. Power Syst.*, vol. 22, no. 4, pp. 2170–2176, Nov. 2007.

[3] Parita G Dalwadi , Chintan R Mehta, "Feasibility Study of Solar-Wind Hybrid Power System", *IEEE Trans. Power Syst.*, Volume 2, Issue 3, March 2012.

[4] Dimitris Ipsakis, Spyros Voutetakis, Panos Seferlis, Fotis Stergiopoulos, Costas Elmasides, "Power management strategies for a stand-alone power system using renewable energy sources and hydrogen storage", *IEEE Trans. Power Syst*, international journal of hydrogen energy 34 (2009)

[5] T. Zhou and B. François, "Energy management and power control of a hybrid active wind generator for distributed power generation and grid integration," *IEEE Trans. Ind. Electron.*, vol. 58, no. 1, pp. 95–104, Jan. 2011

[6] C.Wang andM. H. Nehrir, "Power management of a stand-alone wind/ photovoltaic/fuel cell energy system," *IEEE Trans. Energy Convers.*, vol. 23, no. 3, pp. 957–967, Sep. 2008.

[7] P. Garcia, L.M. Fernandez, C. A. Garcia, and F. Jurado, "Energy management system of fuel-cell-battery hybrid tramway," *IEEE Trans. Ind. Electron.*, vol. 57, no. 12, pp. 4013–4023, Dec. 2010

[8] T.K.A. Brekken,A.Yokochi,A. von Jouanne, Z. Z.Yen,H.M.Hapke, and D. A. Halamay, "Optimal energy storage sizing and control for wind power applications," *IEEE Trans. Sustain. Energy*, vol. 2, no. 1, pp. 69–77, Apr. 2011

[9] A. Hajizadeh, M. A. Golkar, and A. Feliachi, "Voltage control and active power management of hybrid fuel-cell/energy-storage power conversion system under unbalanced voltage sag conditions," *IEEE Trans. Energy Convers.*, vol. 25, no. 4, pp. 1195–1208, Dec. 2010.

[10] C. Wang, M. Nehrir, and S. R. Shaw, "Dynamic models and model validation for PEM fuel cells using electrical circuits," *IEEE Trans. Energy Convers.*, vol. 20, no. 2, pp. 442–451, Jun. 2005

[11] C. Wang, M. Nehrir, and S. R. Shaw, "Dynamic models and model validation for PEM fuel cells using electrical circuits," *IEEE Trans. Energy Convers.*, vol. 20, no. 2, pp. 442–451, Jun. 2005.

[12] T. Zhou, B. Francois, M. el H. Lebbal, and S. Lecoeuche, "Real-time emulation of a hydrogen-production process for assessment of an active wind-energy conversion system," *IEEE Trans. Ind. Electron.*, vol. 56, no. 3, pp. 737–746, Apr. 2009.

[13] K. E. Johnson, L. Y. Pao, M. J. Balas, and L. J. Fingersh, "Control of variable-speed wind turbines: Standard and adaptive techniques for maximizing energy capture," *IEEE Control Syst. Mag.*, vol. 26, no. 3, pp. 70–81, Jun. 2006.

[14] P. C. Klause, O. Wesynczuk, and S. D. Sudhoff, *Analysis of Electric Machinary and Drive System*, 2nd ed. Hoboken, NJ:Wiley, Feb. 2002, 0-471-14326-X.

[15] W. Qiao, L. Qu;, and R. G. Harley, "Control of IMP synchronous generator for maximum wind power generation," *IEEE Trans. Ind. Appl.*, vol. 45, no. 3, pp. 1095–1105, May/Jun. 2009.